

## Outline of Activities Performed During Stage 2

For 2018, 7 tasks were performed, with 3 associated deliverables:

T4. Determining the wavevector components associated with travelling ionospheric disturbances. At this step, the results of previous tasks (T1-T3) were used, first to determine the horizontal components of the plasma density gradients in the time domain:

$$\nabla_x N'_e = \frac{n_x \frac{\partial N'_e}{\partial z}}{\sqrt{1 - n_x^2 - n_y^2}} \quad (1)$$

$$\nabla_y N'_e = \frac{n_y \frac{\partial N'_e}{\partial z}}{\sqrt{1 - n_x^2 - n_y^2}} \quad (2)$$

, where x denotes the zonal (east-west) direction and y the meridional (north-south) direction. Second, the wavevector components are determined in the spectral domain, following the methodology outlined by *Negrea et al. (2016)*:

$$k_z = \frac{\partial \Phi}{\partial z} \quad (3)$$

$$k_x == -i \frac{\nabla_x N'_e}{N'_e} \text{ si } k_y == -i \frac{\nabla_y N'_e}{N'_e} \quad (4)$$

, where  $\Phi$  is the phase obtained through spectral analysis.

T5. Determining the statistical distribution of the TID propagation parameters. Using the results of T4, the statistical distribution of the propagation parameters was determined for each parameter: horizontal wavelength ( $\lambda_h = \frac{2\pi}{\sqrt{k_x^2 + k_y^2}}$ ), vertical wavelength ( $\lambda_z = \left| \frac{2\pi}{k_z} \right|$ ),

propagation direction ( $\theta = \text{atan} \frac{k_y}{k_x}$ ) and the phase speed ( $v_h = \frac{\omega}{\sqrt{k_x^2 + k_y^2}}$ ), separately for

daytime and nighttime intervals. For the daytime data, a clear S-SE propagation direction can be observed (figures 1-2). For the nighttime data, no clear conclusion could be observed, primarily due to the smaller amount of available data (figure 3).

2015 06

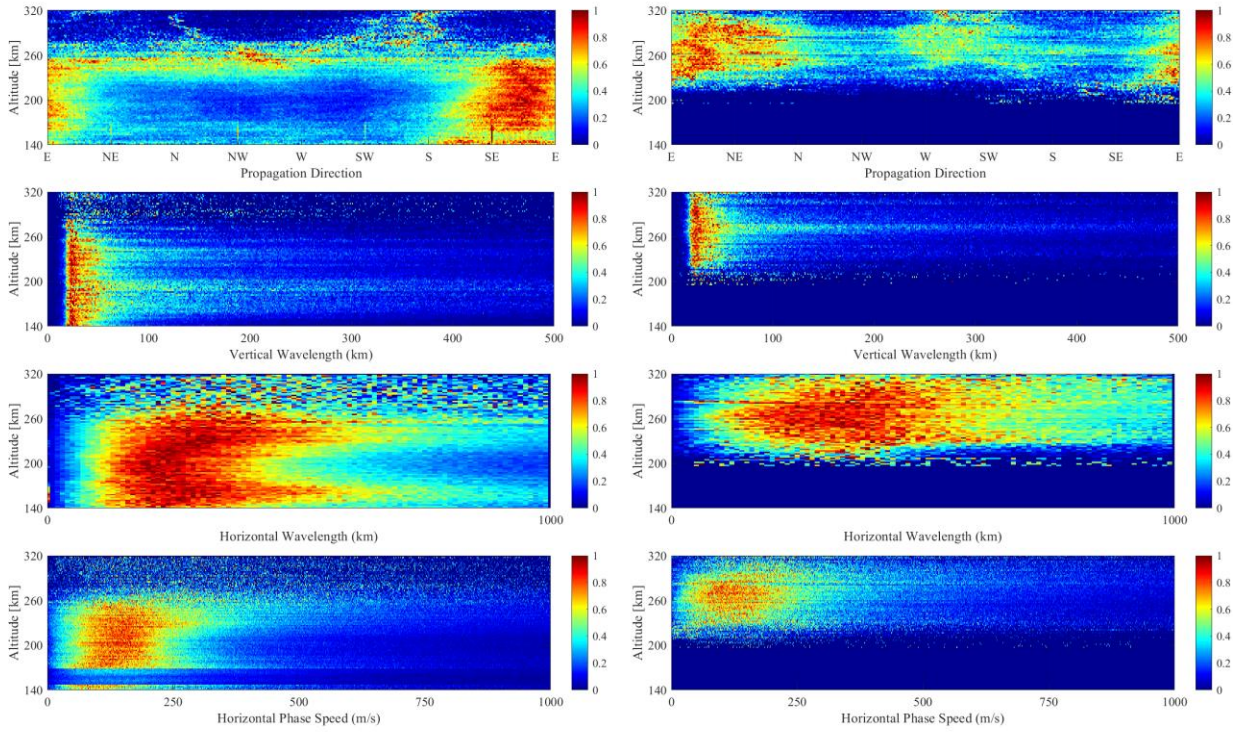


Figure 1. The statistical distribution of the TID propagation parameters for June 2015 at Wallops Island, VA. The left hand column corresponds to daytime data, and the right hand side column to nighttime data.

2015 11

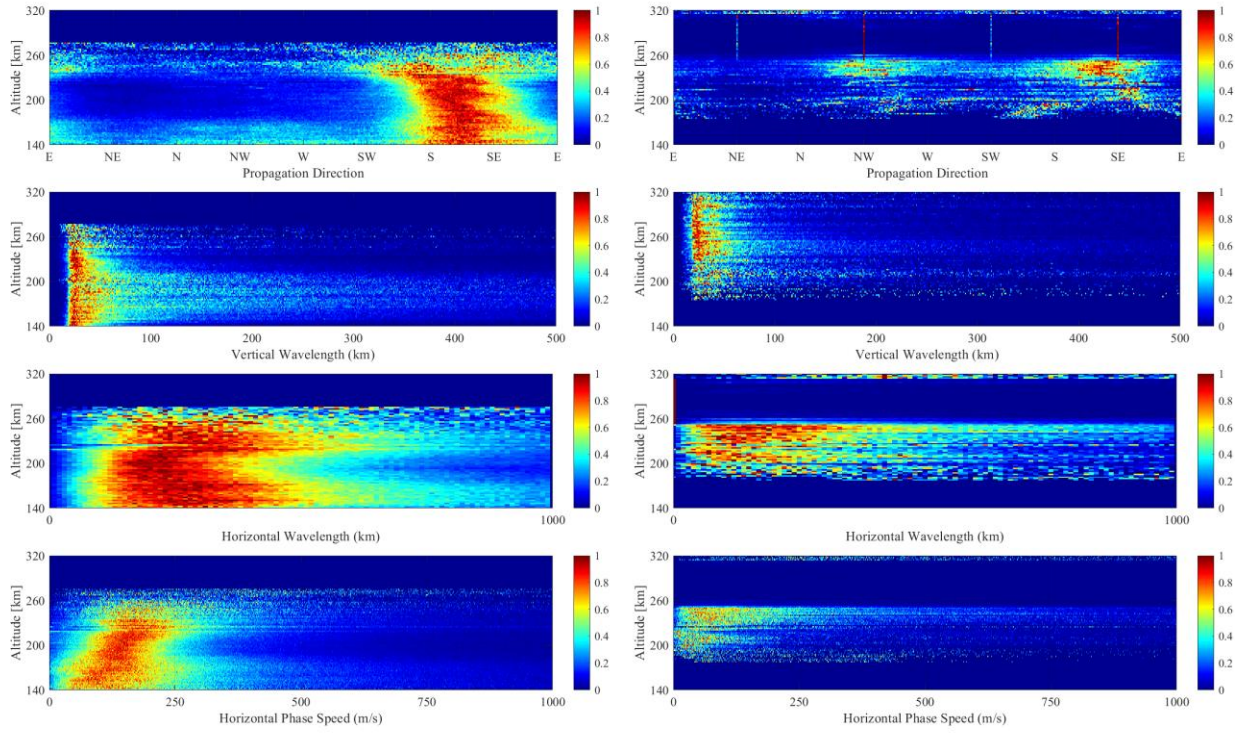


Figure 2. Same as figure 1, but for November 2015.

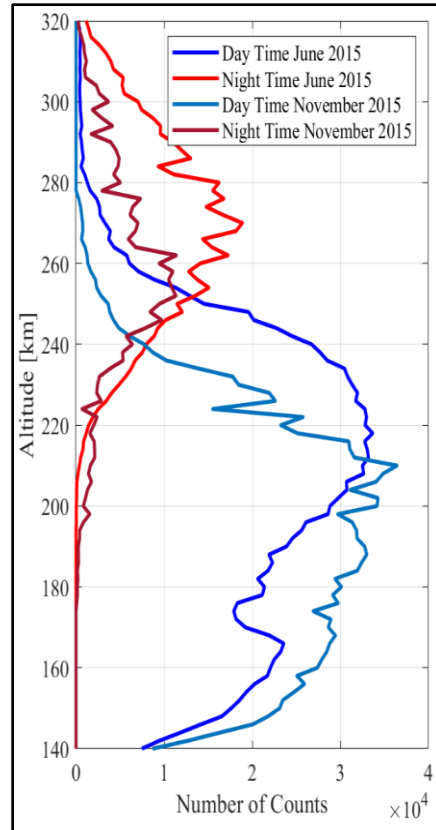


Figure 3. Data availability during June and November 2015, separately for daytime and nighttime.

T6. For this task, the time and altitude variation of the TID parameters was investigated, selecting those parts of the dataset for which a high TID amplitude was observed, simultaneously with stable values for the horizontal and vertical wavelengths and horizontal propagation direction. Figure 4 compares the altitude and temporal variation for these parameters for two frequencies on November 15<sup>th</sup>, one for which a wave packet was present (for those parts of the dataset characterized by high TID amplitude and low variations of the  $\lambda_h$ ,  $\lambda_z$  and  $\theta$ ) and one for which there wasn't.

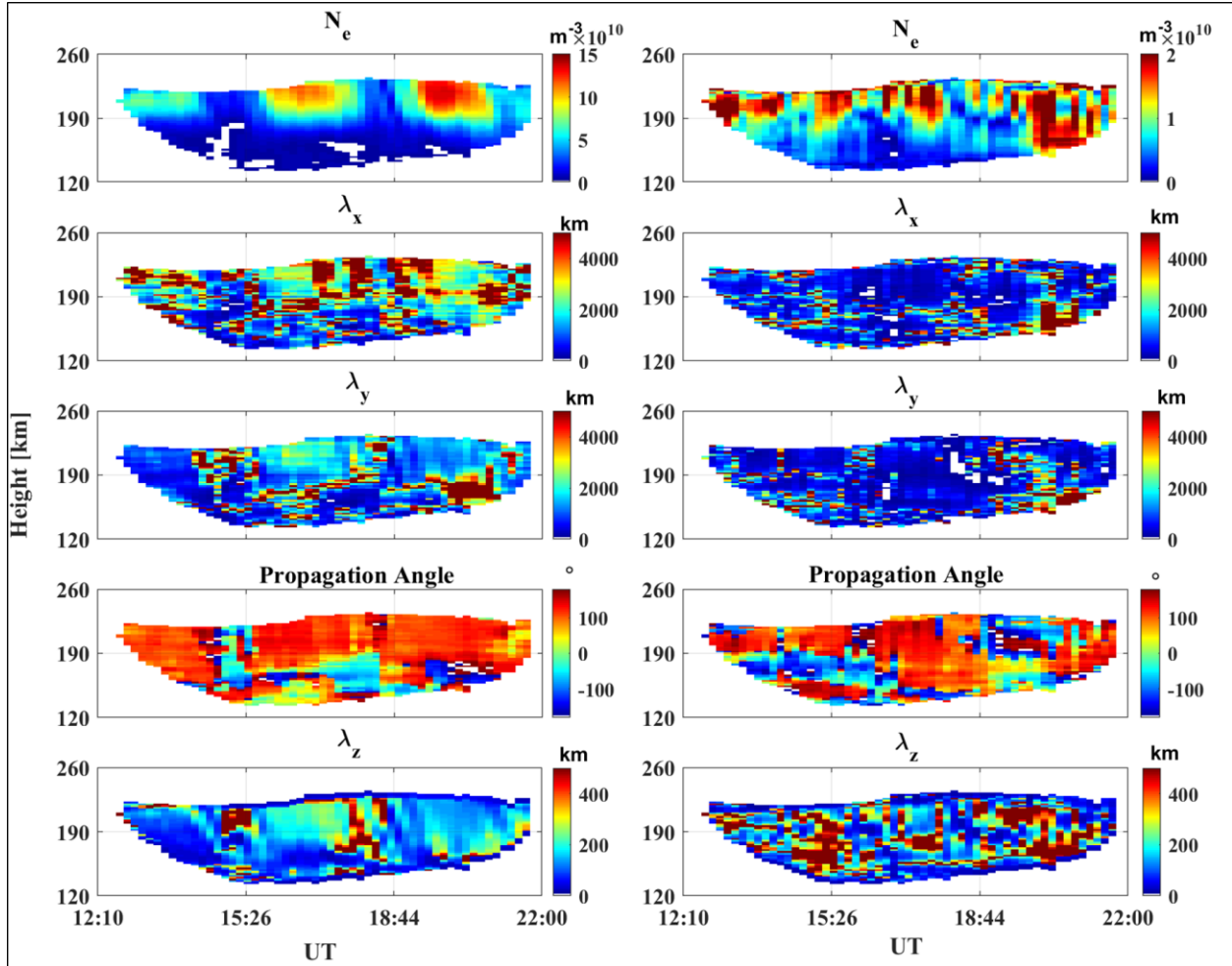


Figure 4. Temporal and height variation of TID parameters at Wallops Island on 15 November 2015. The left hand column corresponds to a frequency of 0.21 mHz (for which wave packets were observed), and the right hand column to a frequency of 0.82 mHz (for which clear wave packets cannot be observed).

T7. An automated algorithm was developed to automatically identify wave packets, based on an image processing technique (Canny, 1986). First, a gaussian filter was applied on each wave parameter obtained as a result of T4 and T6, in order to reduce the impact of erroneous data points. Second, a total gradient is determined for each data point, quantifying the differences to adjacent data points. An example of this result is shown in figure 5. The condition imposed for the detection of a wave packet is a low value for the gradients corresponding to  $\lambda_h$ ,  $\lambda_z$  and  $\theta$ , as well as a high TID amplitude. In practice, all four conditions are satisfied simultaneously in the case of a wave packet.